Electronic Supporting Information

Exploring the oxidation behavior of undiluted and diluted iron particles for energy storage: Mössbauer spectroscopic analysis and kinetic modeling

Jonas Spielmann,[§a] Daniel Braig,[§b] Antonia Streck,[a] Tobias Gustmann,[c,+] Carola Kuhn,[d] Felix Reinauer,[a] Alexandr Kurnosov,[e] Oliver Leubner,[f] Vasily Potapkin,[a] Christian Hasse,[b] Olaf Deutschmann,[c,f] Bastian J.M. Etzold,[g] Arne Scholtissek,[*b] and Ulrike I. Kramm[*a]

[a] Technical University of Darmstadt, Department of Chemistry, Eduard-Zintl-Institute, Otto-Berndt-Str. 3. E-mail: Ulrike.kramm@tu-darmstadt.de,

[b] Technical University of Darmstadt, Department of Mechanical Engineering, Simulation of reactive Thermo-Fluid Systems, Otto-Berndt-Straße 2, 64287 Darmstadt, Germany. E-mail: scholtissek@stfs.tu-darmstadt.de

[c] Leibniz Institute for Solid State and Materials Research Dresden, 01069 Dresden, Germany.

[d] Institute for Chemical Technology and Polymer Chemistry, Karlsruhe Institute of Technology (KIT), Engesserstr.20, Karlsruhe, 76131, Germany

[e] Bayerisches Geoinstitut, University of Bayreuth, Bayreuth, Germany.

[f] Institute of Catalysis Research and Technology, Karlsruhe Institute of Technology (KIT), Hermann-von-Helmholtz-Platz 1, Eggenstein-Leopoldshafen, 76344, Germany

[g] Technical University of Darmstadt, Department of Chemistry, Ernst-Berl-Institute, Peter-Grünberg-Straße 8.

[§] joint first authorship

[+] Present affiliation: OSCAR PLT GmbH, Hamburger Ring 11, Klipphausen/Germany.

Table of Contents

Calculation of sample composition and mass gain.....3

Tables

Table S1: Lamb-Mössbauer factors for iron and its oxides. 3
Table S2: A_i and $xi\%$ for the diluted samples Fe+BN 4
Table S3: A_i and $xi\%$ for the diluted samples Fe+BN 5
Table S4: $ni\%$ and $mi\%$ for the diluted samples Fe+BN 6
Table S5: $ni\%$ and $mi\%$ for the diluted samples Fe+BN 7
Table S6: A_i and $xi\%$ for the undiluted (pure) Fe samples..... 8
Table S7: $ni\%$ and $mi\%$ for the undiluted (pure) Fe samples. 9
Table S8: Mass gain $\Delta m\%$ for the diluted samples Fe+BN. 10
Table S9: Mass gain $\Delta m\%$ for the undiluted (pure) Fe samples. 11
Table S10: Composition of the sieved iron powder from Eckart TLS GmbH (data as provided by the supplier). 12
Table S11: Kinetic parameters for the 600 °C – 700 °C optimization including activation energy and the pre-exponential factor..... 13

Figures

Figure S1: Oxidation of undiluted samples and their characterization via Mössbauer..... 14
Figure S2: Mössbauer spectra of pure iron powder under constant heating of 1 K min^{-1}..... 15
Figure S3: Morphology of Fe+BN mixture before and after oxidation. 16
Figure S4: Mössbauer spectra of pure iron powder oxidized 30 min at 400, 600 & 800 °C.... 17
Figure S5: Mössbauer spectra of the Fe+BN mixtures isothermally oxidized at 600 °C..... 18
Figure S6: Reproducibility check for isothermal oxidation at 600 °C. 19
Figure S7: Mössbauer spectra of the Fe+BN mixtures isothermally oxidized at 633 °C..... 20
Figure S8: Mössbauer spectra of the Fe+BN mixtures isothermally oxidized at 666 °C..... 21
Figure S9: Mössbauer spectra of the Fe+BN mixtures (isothermally oxidized at 700 °C. 22
Figure S10: Mass gain vs square root of oxidation time for isothermal oxidation..... 23
Figure S11: Comparison of the 633 °C - 700°C optimization with that performed for 600 °C - 700°C. 24
Figure S12: Comparison of the 600°C optimization with the 600 °C - 700°C optimization at 600 °C. 25
Figure S13: Comparison of the oxidation behavior of a mono dispersed particle distribution (Sauter mean diameter) with the one of the real particle size distribution..... 26
Figure S14: Particle size over the volume-based probability colored by mass fraction (right) and mass fraction for each particle size (left) (600 °C optimization). 27
Figure S15: Particle size over the volume-based probability colored by mass fraction (633 °C – 700 °C optimization)..... 28
Figure S16: Species mass fraction for each particle size (633°C-700 °C optimization). 29

Calculation of sample composition and mass gain

Extraction of quantitative compositions from Mössbauer spectra is performed according to the following equation

$$x_{i\%} = \frac{\frac{A_i}{f_i}}{\sum_j \frac{A_j}{f_j}} \cdot 100\,,$$

where A_i represents the spectral area of compound *i* and f_i its Lamb-Mössbauer factor. To obtain the number percent $x_{i\%}$ of iron atoms belonging to species *i* the ratio $\frac{A_i}{f_i}$ is divided by the total spectral area, where each sub-spectrum A_j is weighted by their respective LMF f_j. With the stoichiometric coefficients v_i of 1 for Fe and FeO, 3 for Fe_3O_4 and 2 for Fe_2O_3, the number-% of iron atoms can be converted to mol-% according to

$$n_{i\%} = \frac{\frac{x_{i\%}}{v_i}}{\sum_j \frac{x_{j\%}}{v_j}} \cdot 100 = \frac{\frac{x_{i\%}}{v_i}}{x_{Fe\%} + x_{FeO\%} + \frac{x_{Fe3O4\%}}{3} + \frac{x_{Fe2O3\%}}{2}} \cdot 100\,.$$

Further weighting equation 2 with the molar masses M_i of the compounds converts mol-% to mass-% $m_{i\%}$:

$$m_{i\%} = \frac{\frac{x_{i\%}}{v_i} \cdot M_i}{\sum_j (\frac{x_{j\%}}{v_j} \cdot M_j)} \cdot 100$$

From $x_{i\%}$ and the ratio of atoms "O" per atoms "Fe" in a species, the mass gain $\Delta m_{\%}$of a sample can be calculated:

$$\Delta m_{\%} = \frac{(x_{FeO\%} + x_{Fe3O4\%} \cdot \frac{4}{3} + x_{Fe2O3\%} \cdot \frac{3}{2}) \cdot M_O}{M_{Fe}}$$

Lamb-Mössbauer factors used in this work are given in Table S1.

Table S1: Lamb-Mössbauer factors for iron and its oxides.

	LMF	**error**
Fe	0.798	0.01
FeO	0.798	0.01
Fe_3O_4	0.930	0.09
Fe_2O_3	0.840	0.03

The values for $\boldsymbol{A_i}$, $\boldsymbol{x_{i\%}}$, $\boldsymbol{n_{i\%}}$, and $\boldsymbol{m_{i\%}}$ obtained for all samples are presented in Table S4 – S8. Mass gains are summarized in Table S9 and S10.

Table S2: A_i and $x_{i\%}$ for the diluted samples Fe+BN.

A_i									$x_{i\%}$							
T	**oxidation time**	**α-Fe**		**α-Fe_2O_3**		**Fe_3O_4**		**FeO**		**α-Fe**		**α-Fe_2O_3**		**Fe_3O_4**		**FeO**	
			error		error	sum	error		error		error		error	sum	error		error
°C	min					%											
600	0	86.2	1.2	1.0	0.7	10.1	1.5	2.7	0.5	87.5	2.8	1.0	0.7	8.8	6.7	2.7	0.5
	1.5	66.8	1.5	8.9	1.3	21.3	1.7	3.0	0.9	69.2	3.0	8.8	1.2	18.9	4.8	3.1	0.6
	5	59.2	0.9	18.5	0.9	19.2	1.1	3.2	0.6	61.4	2.8	18.2	1.0	17.1	4.3	3.3	0.4
	15	61.1	2.0	24.6	1.5	12.4	3.4	1.9	0.5	63.0	3.0	24.1	1.6	11.0	5.4	2.0	0.3
	30	60.9	1.9	26.7	1.5	10.3	3.4	2.0	0.8	62.7	3.0	26.1	1.6	9.1	5.5	2.1	0.5
	60	56.7	1.7	32.1	1.4	9.1	3.0	2.1	0.5	58.4	2.9	31.4	1.6	8.0	5.1	2.2	0.3
	120	49.5	0.9	33.8	0.8	13.1	1.2	3.6	0.7	51.3	2.9	33.3	1.2	11.7	3.9	3.7	0.4
	180	42.3	1.0	36.9	1.0	16.4	1.4	4.4	0.9	44.1	3.1	36.6	1.4	14.7	3.3	4.6	0.4
	240	43.9	0.6	38.1	0.6	14.8	0.9	3.3	0.3	45.7	2.8	37.7	1.1	13.2	3.4	3.4	0.1
	360	45.3	1.3	34.8	1.3	16.4	2.0	3.5	0.6	47.2	3.0	34.5	1.5	14.7	3.7	3.6	0.3
	360	30.9	0.6	42.2	0.7	22.2	1.0	4.8	0.9	32.6	3.1	42.3	1.4	20.1	2.3	5.1	0.3
	360	40.1	1.2	44.8	1.3	12.5	2.0	2.6	0.6	41.8	3.1	44.4	1.6	11.2	3.5	2.7	0.3
	1440	15.4	0.6	59.4	0.7	21.8	0.9	3.4	0.3	16.4	3.2	60.1	1.6	19.9	1.4	3.6	0.1
	1440	22.0	0.7	63.0	0.9	13.4	1.2	1.6	0.4	23.2	4.5	63.0	1.5	12.1	2.0	1.7	0.1
	360	34.7	0.7	41.2	0.8	22.1	1	2	0.4	36.6	2.8	41.3	1.4	20.0	2.6	2.1	0.2
	360	25.7	0.4	47.7	0.5	22	0.7	4.6	0.4	27.2	3.1	48.0	1.4	20.0	1.9	4.9	0.1
400	30	97.7	2.3	0.8	1.1	1.6	2.9	0.0	0.0	97.9	2.6	0.7	1.0	1.3	8.4	0.0	0.0
800	30	0.0	0.0	91.4	2.0	8.6	1.9	0.0	0.0	0.0	0.0	92.2	1.8	7.8	1.6	0.0	0.0

Table S3: A_i and $x_{i\%}$ for the diluted samples Fe+BN.

A_i									$x_{i\%}$							
T	**oxidation time**	**α-Fe**		**α-Fe_2O_3**		**Fe_3O_4**		**FeO**		**α-Fe**		**α-Fe_2O_3**		**Fe_3O_4**		**FeO**	
			error		error	sum	error		error		error		error	sum	error		error
°C	min					%											
633	20	34.9	2.8	29.3	2.5	26.3	11.1	9.6	1.0	36.8	5.9	29.3	3.7	23.8	8.1	10.1	0.4
	30	25.6	2.2	41.4	3.4	23.2	12.0	9.7	1.0	27.1	4.9	41.6	5.2	21.0	8.8	10.3	0.3
	60	16.1	2.2	51.4	5.7	25.6	15.8	6.9	1.2	17.1	4.1	52.1	8.3	23.4	11.2	7.3	0.2
	120	11.9	0.9	58.3	1.5	23.3	2.6	6.5	0.7	12.6	2.6	59.0	2.3	21.3	2.1	7.0	0.1
	360	4.3	0.6	73.5	1.1	20.0	1.6	2.2	0.4	4.6	2.4	74.7	1.9	18.3	1.3	2.3	0.0
666	20	11.5	1.2	44.5	1.6	27.7	2.9	16.3	0.8	12.3	2.7	45.0	2.2	25.4	2.2	17.4	0.1
	30	12.4	1.2	36.5	2.6	30.5	5.2	20.6	1.5	13.2	3.4	37.0	2.9	27.9	3.7	22.0	0.2
	60	7.6	1.0	48.8	3.0	27.4	5.1	16.2	1.1	8.1	2.0	49.5	3.3	25.1	3.6	17.3	0.1
	120	3.2	0.6	68.0	5.7	20.0	1.9	8.8	0.8	3.4	1.3	68.9	2.7	18.3	1.9	9.4	0.0
	360	0.0	0.0	87.7	1.4	10.5	2.1	1.9	0.5	0.0	0.0	88.5	2.0	9.5	1.7	2.0	0.0
700	20	2.8	1.3	53.6	4.6	30.6	12.1	13.1	1.2	3.0	1.5	54.7	6.8	28.2	8.1	14.1	0.0
	30	2.1	0.9	58.8	4.1	30.7	10.0	8.4	0.8	2.3	1.2	60.2	6.2	28.4	6.8	9.1	0.0
	60	0.0	0.0	71.4	1.2	24.3	1.9	4.3	0.5	0.0	0.0	73.0	2.2	22.4	1.5	4.6	0.0
	120	0.0	0.0	90.2	1.5	9.8	2.3	0.0	0.0	0.0	0.0	91.0	2.1	9.0	1.9	0.0	0.0
	240	0.0	0.0	100.0	0.0	0.0	0.0	0.0	0.0	0.0	0.0	100.0	0.0	0.0	0.0	0.0	0.0

Table S4: $n_{i\%}$ and $m_{i\%}$ for the diluted samples Fe+BN.

		$n_{i\%}$								$m_{i\%}$							
T	**oxidation time**	**α-Fe**		**α-Fe_2O_3**		**Fe_3O_4**		**FeO**		**α-Fe**		**α-Fe_2O_3**		**Fe_3O_4**		**FeO**	
			error		error	sum	error		error		error		error	sum	error		error
°C	min					%											
600	0	93.4	3.0	0.5	0.4	3.1	2.4	2.9	0.5	83.8	2.7	1.3	0.9	11.6	8.9	3.3	0.5
	1.5	83.4	3.6	5.3	0.7	7.6	1.9	3.7	0.8	61.9	2.7	11.2	1.6	23.4	6.0	3.4	0.7
	5	77.2	3.5	11.5	0.6	7.2	1.8	4.2	0.5	53.3	2.4	22.6	1.2	20.5	5.2	3.6	0.4
	15	78.1	3.7	14.9	1.0	4.5	2.2	2.4	0.4	54.7	2.6	30.0	2.0	13.2	6.5	2.1	0.4
	30	77.5	3.7	16.2	1.0	3.8	2.3	2.5	0.7	54.4	2.6	32.4	2.0	10.9	6.6	2.2	0.6
	60	74.0	3.6	19.9	1.0	3.4	2.1	2.7	0.4	49.9	2.4	38.4	2.0	9.5	6.0	2.3	0.3
	120	67.9	3.8	22.0	0.8	5.1	1.7	4.9	0.5	42.9	2.4	39.8	1.4	13.5	4.5	3.9	0.4
	180	61.4	4.4	25.4	1.0	6.8	1.5	6.4	0.6	36.0	2.6	42.7	1.6	16.6	3.8	4.6	0.4
	240	63.1	3.9	26.0	0.8	6.1	1.6	4.7	0.2	37.4	2.3	44.1	1.3	15.0	3.8	3.5	0.1
	360	64.7	4.1	23.6	1.0	6.7	1.7	5.0	0.4	38.9	2.5	40.6	1.8	16.7	4.2	3.7	0.3
	360	49.8	4.7	32.3	1.1	10.2	1.2	7.7	0.5	25.6	2.4	47.6	1.6	21.9	2.5	4.9	0.3
	360	59.3	4.4	31.5	1.1	5.3	1.6	3.8	0.4	33.7	2.5	51.1	1.9	12.5	3.9	2.7	0.3
	1440	28.9	5.6	53.0	1.4	11.7	0.8	6.4	0.1	12.2	2.4	64.0	1.7	20.5	1.4	3.3	0.0
	1440	38.3	7.5	52.2	1.2	6.7	1.1	2.8	0.2	17.5	3.4	68.2	1.6	12.7	2.1	1.6	0.1
	360	55.4	4.3	31.3	1.0	10.1	1.3	3.2	0.2	29.1	2.3	46.9	1.6	22.0	2.8	2.1	0.2
	360	43.4	4.9	38.3	1.1	10.6	1.0	7.8	0.2	21.0	2.4	53.0	1.5	21.3	2.0	4.7	0.1
400	30	99.2	2.7	0.4	0.5	0.5	2.8	0.0	0.0	97.2	2.6	1.0	1.4	1.8	11.5	0.0	0.0
800	30	0.0	0.0	94.6	1.8	5.4	1.1	0.0	0.0	0.0	0.0	92.4	1.8	7.6	1.6	0.0	0.0

Table S5: $n_{i\%}$ and $m_{i\%}$ for the diluted samples Fe+BN.

$n_{i\%}$										$m_{i\%}$							
T	**oxidation time**	**α-Fe**		**α-Fe_2O_3**		**Fe_3O_4**		**FeO**		**α-Fe**		**α-Fe_2O_3**		**Fe_3O_4**		**FeO**	
			error		error	sum	error		error		error		error	sum	error		error
°C	min					%											
633	20	52.9	8.5	21.1	2.7	11.4	3.9	14.5	0.5	29.6	4.8	33.8	4.3	26.5	9.0	10.1	0.4
	30	41.5	7.6	31.9	4.0	10.8	4.5	15.8	0.4	21.1	3.8	46.3	5.8	22.7	9.5	9.9	0.3
	60	29.3	7.1	44.7	7.1	13.4	6.4	12.6	0.3	12.9	3.1	56.0	8.9	24.3	11.7	6.8	0.2
	120	22.5	4.7	52.5	2.0	12.6	1.3	12.4	0.1	9.4	1.9	62.4	2.4	21.8	2.2	6.4	0.1
	360	9.2	4.8	74.1	1.9	12.1	0.9	4.6	0.0	3.3	1.7	76.5	2.0	18.1	1.3	2.1	0.0
666	20	20.2	4.5	37.1	1.8	14.0	1.2	28.7	0.1	9.2	2.1	48.3	2.4	26.3	2.3	16.2	0.1
	30	20.9	5.3	29.4	2.3	14.8	2.0	34.9	0.3	10.0	2.6	40.1	3.1	29.2	3.9	20.7	0.2
	60	13.8	3.5	42.3	2.8	14.3	2.1	29.6	0.1	6.0	1.5	52.4	3.5	25.7	3.7	15.9	0.1
	120	6.3	2.5	64.6	2.6	11.4	1.2	17.7	0.1	2.4	1.0	71.0	2.8	18.2	1.9	8.4	0.0
	360	0.0	0.0	89.5	2.0	6.4	1.2	4.1	0.0	0.0	0.0	89.0	2.0	9.3	1.7	1.7	0.0
700	20	5.5	2.9	50.8	6.3	17.5	5.0	26.1	0.1	2.2	1.1	56.8	7.0	28.4	8.2	12.7	0.0
	30	4.5	2.3	59.1	6.0	18.6	4.4	17.8	0.0	1.6	0.8	62.0	6.3	28.3	6.7	8.1	0.0
	60	0.0	0.0	75.2	2.3	15.4	1.0	9.4	0.0	0.0	0.0	74.0	2.3	22.0	1.5	4.0	0.0
	120	0.0	0.0	93.8	2.1	6.2	1.3	0.0	0.0	0.0	0.0	91.3	2.1	8.7	1.9	0.0	0.0
	240	0.0	0.0	100.0	0.0	0.0	0.0	0.0	0.0	0.0	0.0	100.0	0.0	0.0	0.0	0.0	0.0

Table S6: A_i and $x_{i\%}$ for the undiluted (pure) Fe samples.

A_i									$x_{i\%}$							
T	**oxidation time**	**α-Fe**		**α-Fe_2O_3**		**Fe_3O_4**		**FeO**		**α-Fe**		**α-Fe_2O_3**		**Fe_3O_4**		**FeO**	
			error		error	sum	error		error		error		error	sum	error		error
°C	min					%											
400	30	95.6	1.0	1.9	0.7	2.4	0.9	0.0	0.0	96.1	1.0	1.8	0.7	2.1	7.9	0.0	0.0
600	30	46.0	1.0	20.9	1.0	30.3	1.3	2.8	0.7	48.6	2.8	21.0	1.2	27.5	3.1	3.0	0.3
800	30	22.1	1.2	22.9	1.3	20.4	1.8	34.6	1.0	23.0	8.4	22.7	1.5	18.3	2.1	36.1	0.2
RT	heating rate: 1 K min^{-1}	100	0	0	0	0	0	0	0	100.0	0.0	0.0	0.0	0.0	8.3	0.0	0.0
100		100	0	0	0	0	0	0	0	100.0	0.0	0.0	0.0	0.0	8.3	0.0	0.0
200		100	0	0	0	0	0	0	0	100.0	0.0	0.0	0.0	0.0	8.3	0.0	0.0
300		100	1.9	0	0	0	0	0	0	100.0	0.0	0.0	0.0	0.0	8.3	0.0	0.0
400		95.6	1.2	1.5	1	3	1.1	0	0	96.0	1.3	1.4	0.9	2.6	7.8	0.0	0.0
450		88.1	1.5	3.4	1.2	8.5	1.5	0	0	89.3	1.7	3.3	1.1	7.4	7.0	0.0	0.0
500		63.9	2	22.2	1.6	13.9	2.9	0	0	65.9	2.6	21.8	1.6	12.3	5.3	0.0	0.0
550		47.5	1.1	12	1.1	40.4	2	0	0	50.8	2.7	12.2	1.2	37.1	3.0	0.0	0.0
600		22.9	0.5	34.7	0.6	42.3	0.9	0	0	24.8	2.5	35.8	1.7	39.4	1.5	0.0	0.0

Table S7: $n_{i\%}$ and $m_{i\%}$ for different oxidation treatments of the undiluted (pure) Fe samples.

$n_{i\%}$									$m_{i\%}$							
T	**oxidation time**	**α-Fe**		**α-Fe_2O_3**		**Fe_3O_4**		**FeO**		**α-Fe**		**α-Fe_2O_3**		**Fe_3O_4**		**FeO**	
			error		error	sum	error		error		error		error	sum	error		error
°C	min					%											
400	30	98.3	1.1	0.9	0.3	0.7	2.7	0.0	0.0	94.6	1.0	2.6	1.0	2.9	10.7	0.0	0.0
600	30	68.2	3.9	14.7	0.8	12.9	1.4	4.2	0.5	40.4	2.3	24.9	1.4	31.6	3.6	3.1	0.3
800	30	30.1	11.0	14.8	1.0	8.0	0.9	47.1	0.2	18.4	6.7	25.9	1.7	20.1	2.4	35.7	0.2
RT	heating rate: 1 K min^{-1}	100.0	0.0	0.0	0.0	0.0	2.8	0.0	0.0	100.0	0.0	0.0	0.0	0.0	11.5	0.0	0.0
100		100.0	0.0	0.0	0.0	0.0	2.8	0.0	0.0	100.0	0.0	0.0	0.0	0.0	11.5	0.0	0.0
200		100.0	0.0	0.0	0.0	0.0	2.8	0.0	0.0	100.0	0.0	0.0	0.0	0.0	11.5	0.0	0.0
300		100.0	0.0	0.0	0.0	0.0	2.8	0.0	0.0	100.0	0.0	0.0	0.0	0.0	11.5	0.0	0.0
400		98.4	1.3	0.7	0.5	0.9	2.7	0.0	0.0	94.5	1.3	2.0	1.3	3.5	10.6	0.0	0.0
450		95.6	1.8	1.8	0.6	2.6	2.5	0.0	0.0	85.7	1.6	4.5	1.5	9.8	9.3	0.0	0.0
500		81.5	3.2	13.5	1.0	5.1	2.2	0.0	0.0	57.8	2.3	27.3	2.0	14.9	6.4	0.0	0.0
550		73.3	3.8	8.8	0.8	17.9	1.4	0.0	0.0	42.5	2.2	14.6	1.4	42.9	3.4	0.0	0.0
600		44.5	4.5	32.0	1.5	23.5	0.9	0.0	0.0	19.0	1.9	39.2	1.8	41.7	1.6	0.0	0.0

Table S8: Mass gain $\Delta m_{\%}$ for diluted samples Fe+BN.

T	oxidation time	mass gain	
		%	error
°C	min		
600	0	4.6	3.0
	1.5	11.9	2.6
	5	15.3	2.2
	15	15.1	2.8
	30	15.3	2.9
	60	17.2	2.7
	120	19.8	2.1
	180	22.7	2.0
	240	22.2	1.8
	360	21.5	2.1
	360	27.3	1.6
	360	24.1	2.1
	1440	34.5	1.2
	1440	32.2	1.4
	360	26.0	1.6
	360	29.6	1.4
400	30	0.8	3.6
800	30	42.6	1.4
633	20	24.6	4.8
	30	28.9	5.7
	60	33.4	7.9
	120	35.5	1.8
	360	39.8	1.3
666	20	34.0	1.8
	30	32.8	2.7
	60	35.8	2.8
	120	39.3	1.9
	360	42.2	1.5
700	20	38.3	6.0
	30	39.3	5.2
	60	41.2	1.5
	120	42.5	1.6
	240	43.0	0.0

Table S9: Mass gain $\Delta m_{\%}$ for undiluted, pure Fe samples.

T	**oxidation time**	**mass gain**	
		%	error
°C	min		
400	30	1.6	3.3
600	30	20.4	1.8
800	30	27.0	1.5
RT	heating rate: 1 K min^{-1}	0.0	3.2
100		0.0	3.2
200		0.0	3.2
300		0.0	3.2
400		1.6	3.4
450		4.2	3.2
500		14.1	2.7
550		19.4	1.6
600		30.4	1.3

Iron Powder composition

Table S10: Composition of the sieved iron powder from Eckart TLS GmbH (data as provided by the supplier).

Element	Fe	Si	C	Mn	Cr	Ni
wt.-%	99.8	0.011	0.007	0.017	0.013	0.011

Kinetic parameters for the 600 °C – 700 °C optimization

Table S11: Kinetic parameters for the 600 °C – 700 °C optimization including activation energy and the pre-exponential factor; values are extracted considering all four temperature data sets. See main manuscript for the more accurate fitting.

Reaction	$k_{x,}^{'0}$ / m² s⁻¹	E_a / J mol⁻¹
$Fe + {}^1/_2O_2 \rightarrow FeO$	$1.93*10^{-4}$	203069
$3FeO + {}^1/_2O_2 \rightarrow Fe_3O_4$	$2.76 * 10^{-5}$	181596
$2Fe_3O_4 + {}^1/_2O_2 \rightarrow 3Fe_2O_3$	$5 * 10^{-4}$	205398

Oxidation process for the pure iron powder and composition during oxidation under constant heating

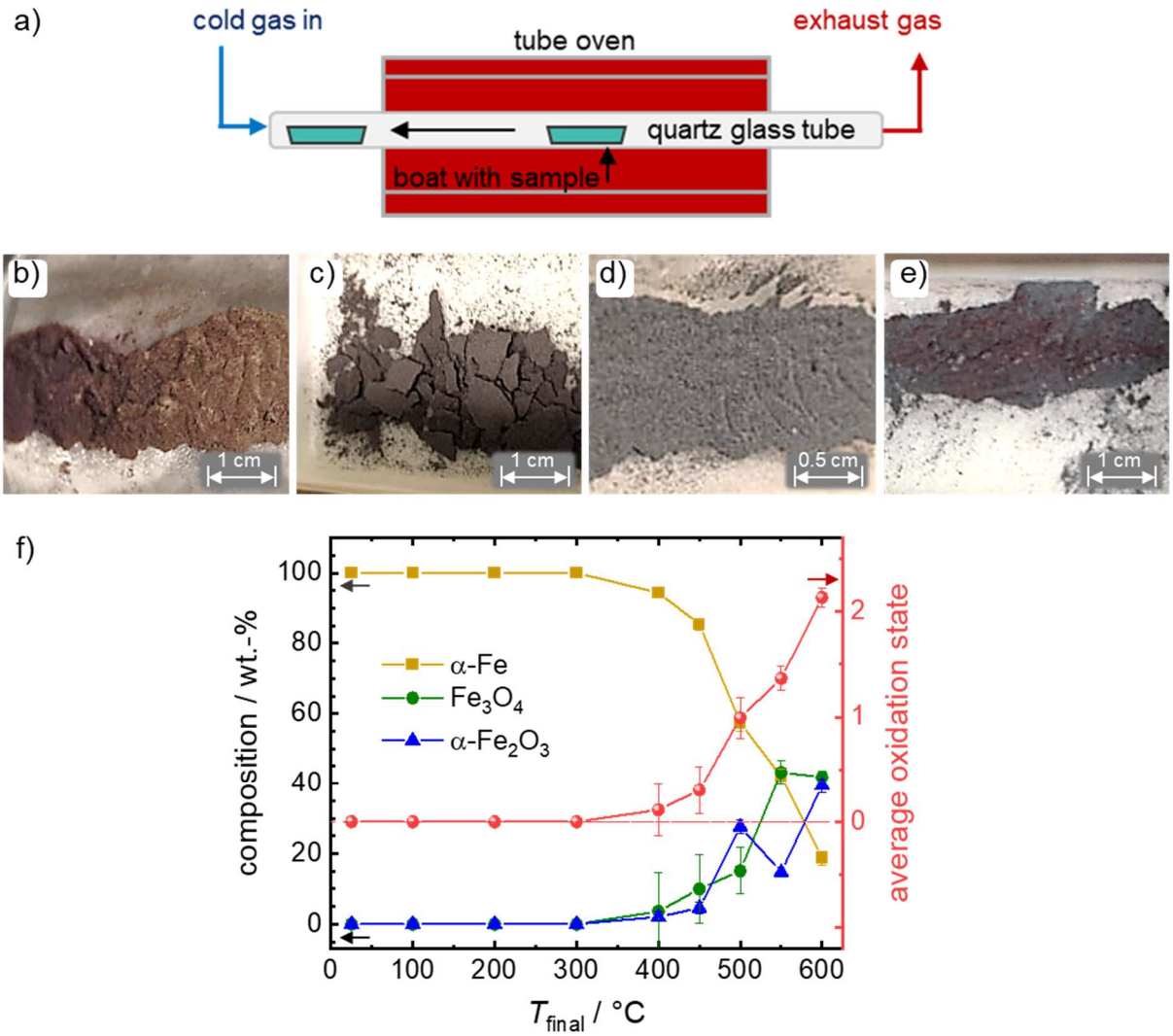

Figure S1: Scheme of the tube furnace used for the oxidation processes (a). b) - e) Photographs of the samples obtained from oxidation under constant heating in a tube oven with 1 K min^{-1} up to 300 °C (b), 400 °C (c), 600 °C (d) and 800 °C (e) and iron-related composition obtained from Mössbauer spectroscopy (f). The composition in wt.-% is given on the left axis while the right axis reports the average oxidation state.

Mössbauer spectra of undiluted iron powder heated in air to the given temperatures

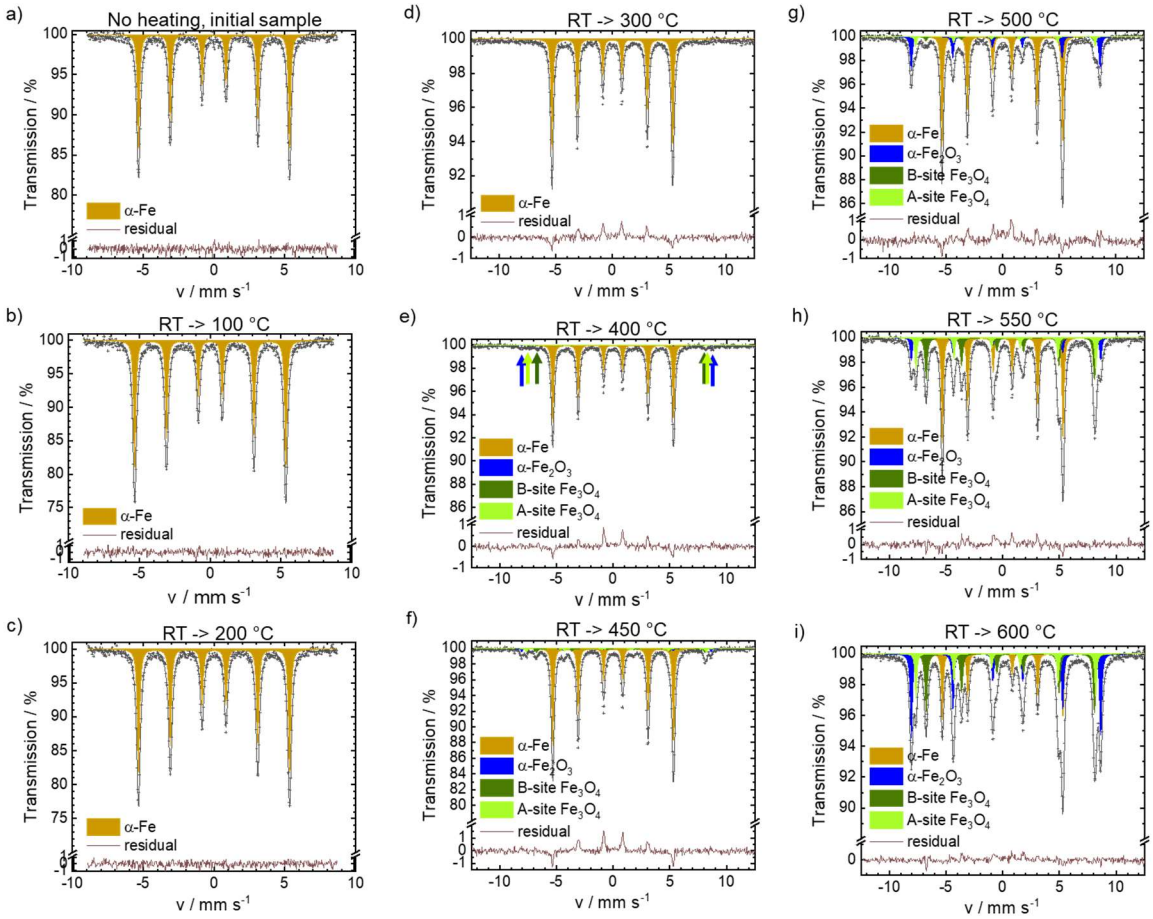

Figure S2: Mössbauer spectra of pure iron powder, oxidized in a Carbolite tube oven, all samples are directly heated under compressed air from RT to the indicated temperature with a heating ramp of 1 K min^{-1}.

Sample morphology of diluted iron powder

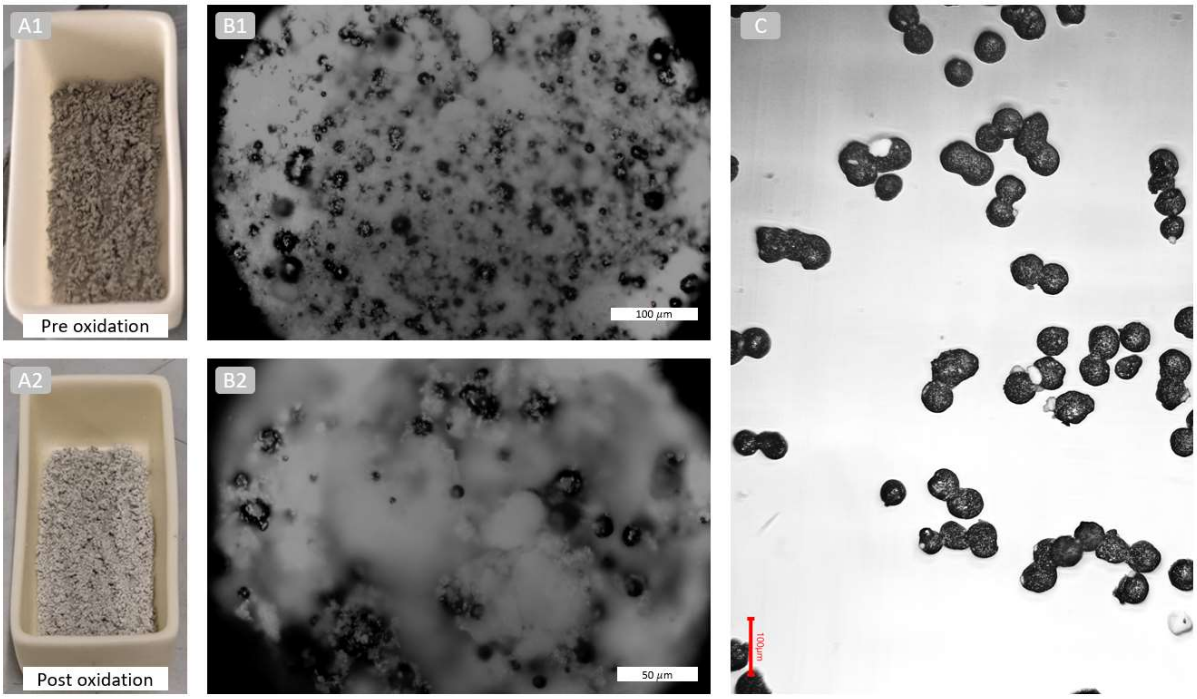

Figure S3: Fe+BN mixture with 70 wt-% Fe, oxidized at 600°C for 3 h. (A) Photographs of the samples pre and post oxidation. A powder is maintained. (B) Microscope images of diluted samples after the oxidation. (C) Oxidized sample after removing boron nitride. Only linear agglomerates can be identified, while most of the particles remains separated. This is taken as successful suppression of the sintering process.

Isothermal oxidation of undiluted iron powders

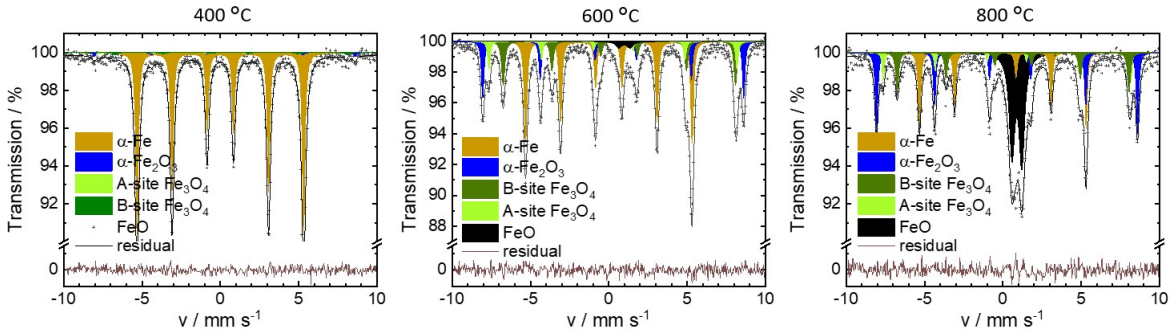

Figure S4: Mössbauer spectra of pure iron powder oxidation. Samples were heated under N_2 to 400, 600 & 800 °C and then oxidized in pressured air for the indicated oxidation times.

Note, that preparation of a sample for T > 600 °C for Mössbauer spectroscopy is possible in this case as the sample was grindable. We assume this is due to overall shorter reaction time, as for samples previously obtained under constant heating rate (heating with 1 K min^{-1} to T > 600 °C takes > 10 h).

Mössbauer spectra of diluted iron powders – 600 °C

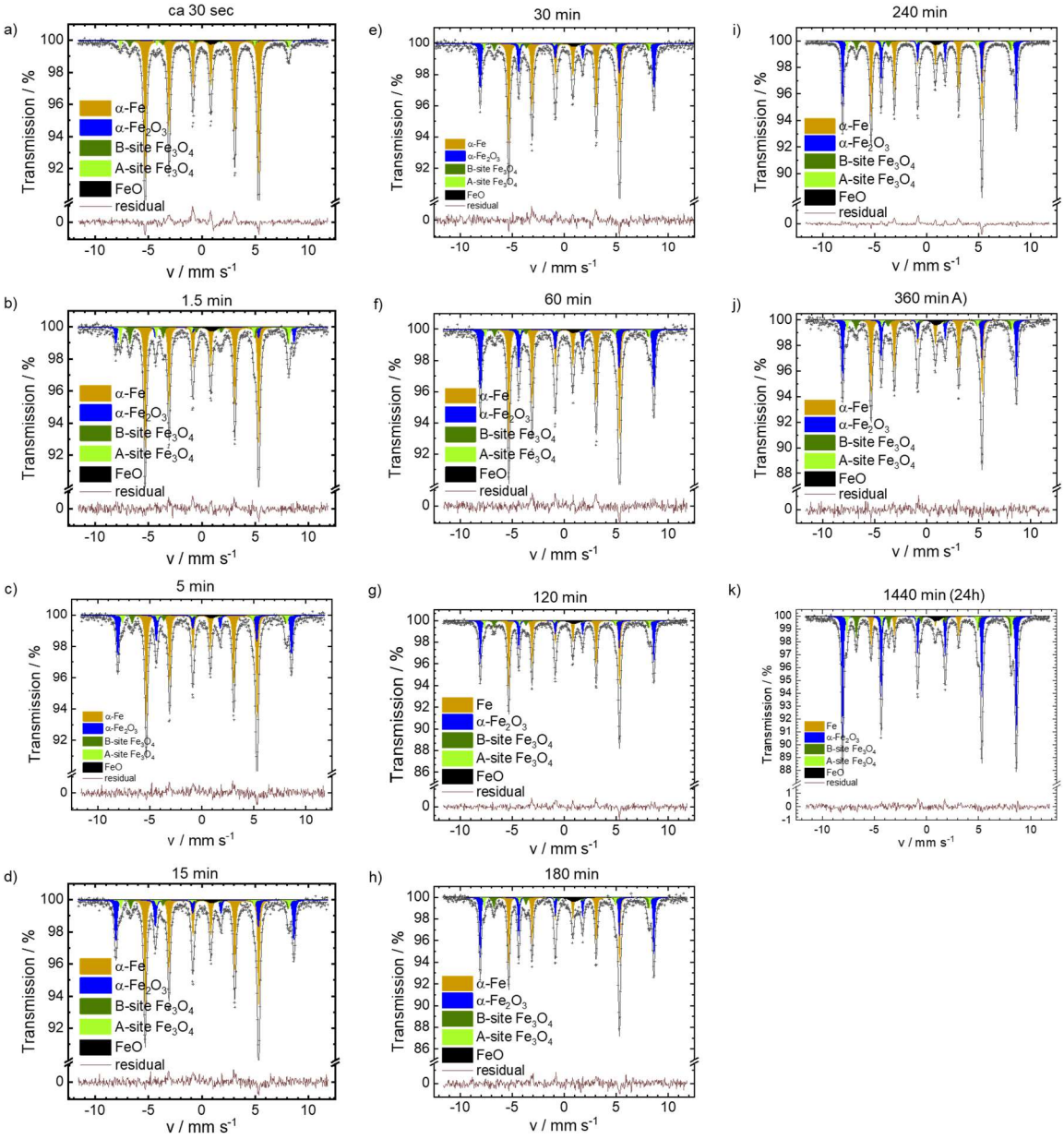

Figure S5: Mössbauer spectra of the Fe+BN mixtures (70 wt. % Fe). Samples are heated under N_2 to 600 °C and then oxidized in pressured air for the indicated oxidation times, with one exception: Sample (a) is removed from oven under inert conditions. Contact with air happened only after the sample is pushed out of the oven for cooling down.

Reproducibility check (600 °C, 360 min)

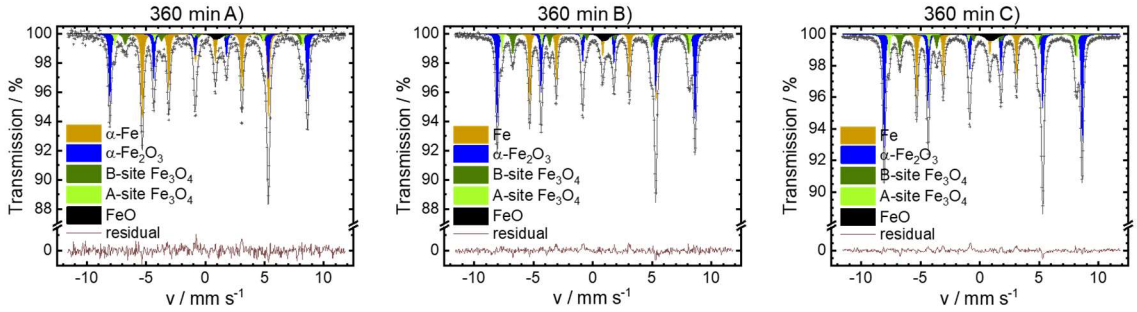

Figure S6: Mössbauer spectra to check for reproducibility of the experiments. All samples were obtained from an oxidative treatment at 600 °C for 360 min.

Mössbauer spectra of diluted iron powders - 633 °C

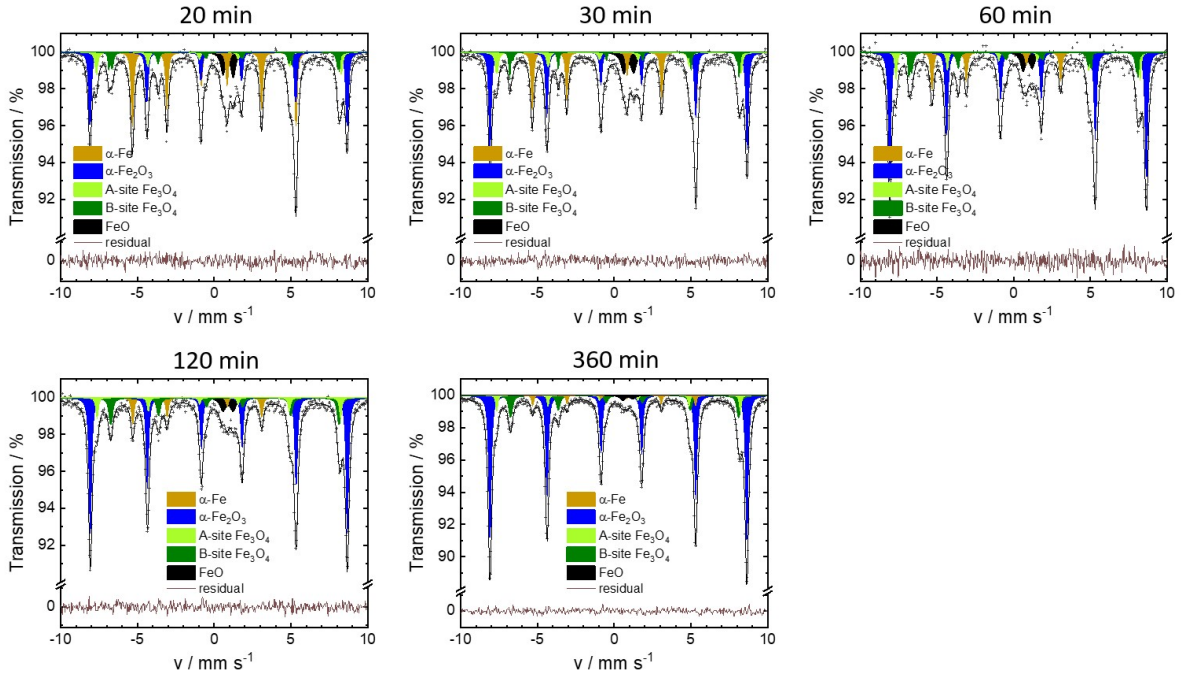

Figure S7: Mössbauer spectra of the Fe+BN mixtures (70 wt. % Fe). Samples are heated under N_2 to 633 °C and then oxidized in pressured air for the indicated oxidation times.

Mössbauer spectra of diluted iron powders - 666 °C

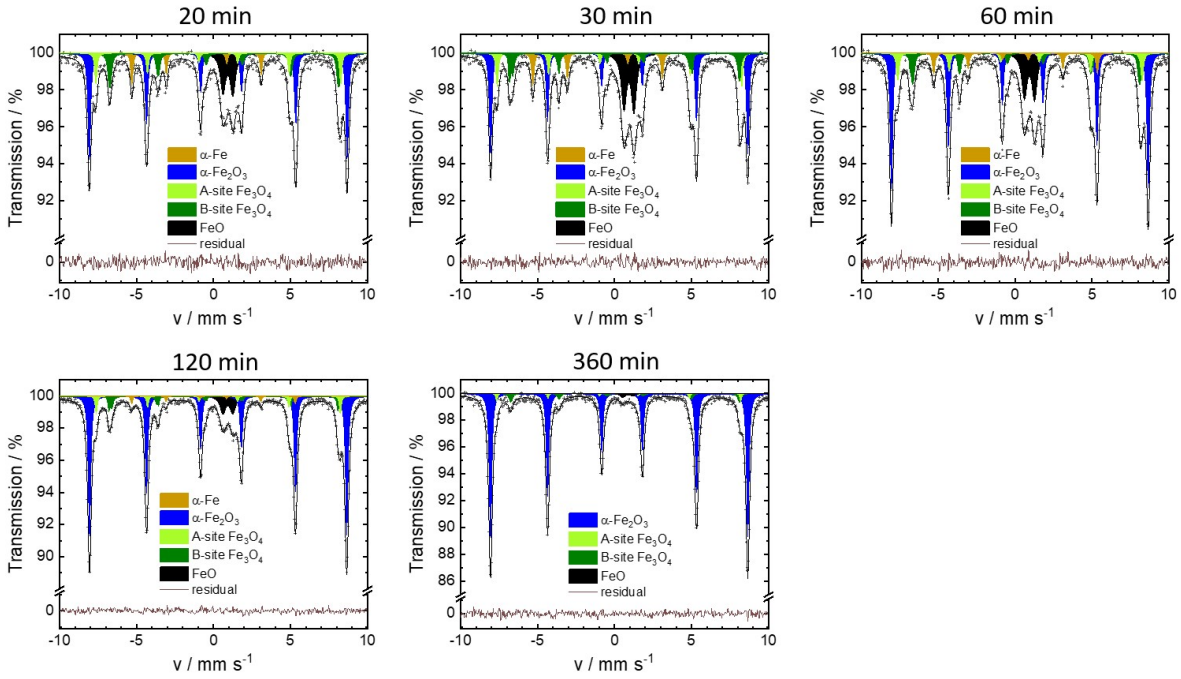

Figure S8: Mössbauer spectra of the Fe+BN mixtures (70 wt. % Fe). Samples are heated under N_2 to 666 °C and then oxidized in pressured air for the indicated oxidation times.

Mössbauer spectra of diluted iron powders - 700 °C

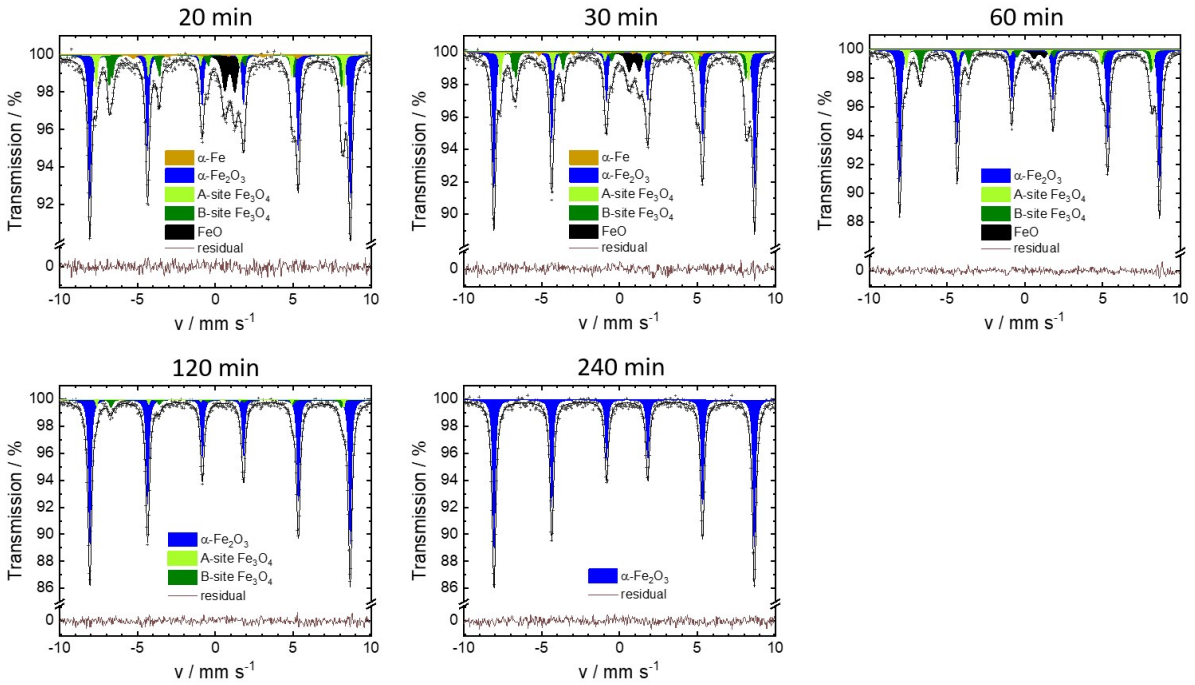

Figure S9: Mössbauer spectra of the Fe+BN mixtures (70 wt. % Fe). Samples are heated under N_2 to 700 °C and then oxidized in pressured air for the indicated oxidation times.

Comparison of mass gain for oxidation between 600 °C – 700 °C

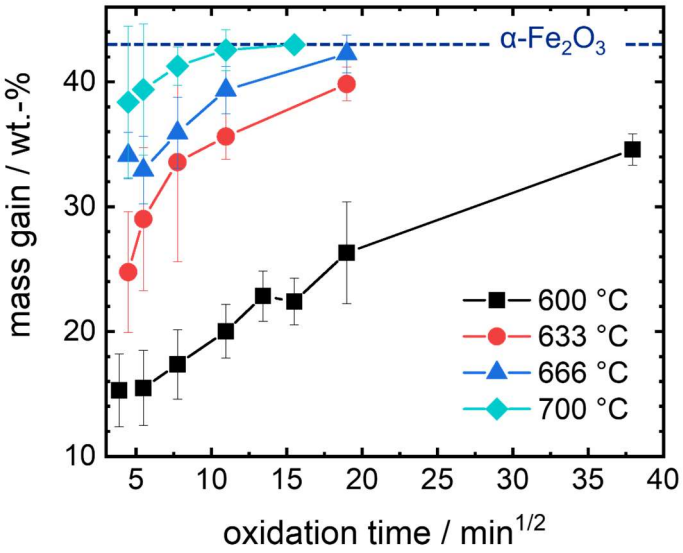

Figure S10: Mass gain vs square root of oxidation time as obtained from isothermal oxidation at the indicated temperatures for the diluted Fe+BN system. Mass gain represents the amount of oxygen incorporated in the sample as compared to initial weight of iron. In classic bulk iron oxidation, after a kinetically limited fast initial oxidation stage, mass gain during isothermal oxidation follows a parabolic rate law and thus should produce a straight line in the figure. Deviations from this behavior is due to the influence of particle geometry and a particle size distribution: Small particles are already fully oxidized to Fe_2O_3 at short oxidation times, while larger particles still have lesser oxides remaining in the core. Since a portion of particles can't contribute anymore to the oxidation, the mass gain slows down. The fact that the inner layers of a particle also contain weight-wise less iron than the outer layers also contributes to this phenomenon.

Comparison of the 633 °C - 700°C optimization under consideration of the overall data sets at 600 °C -700°C

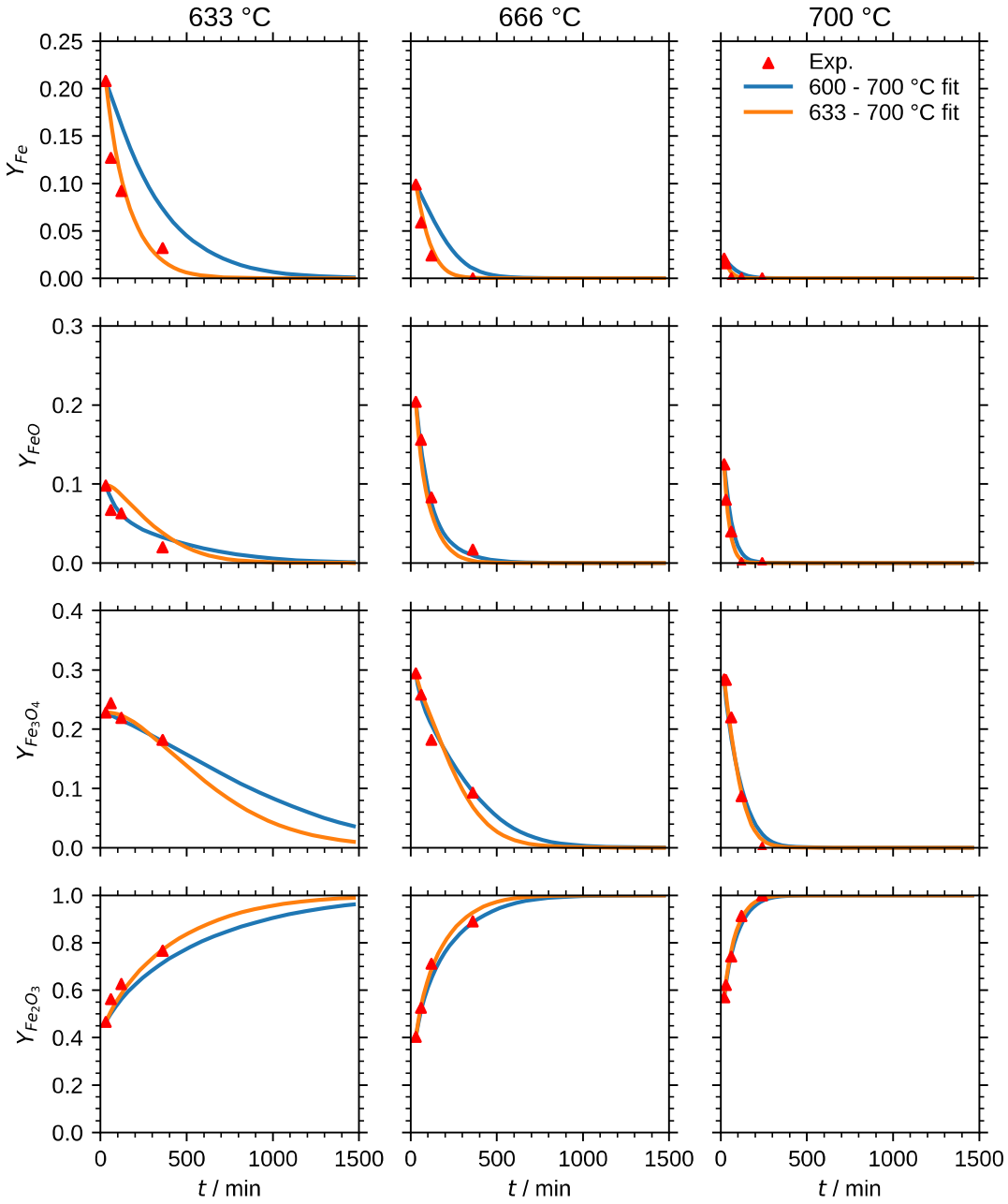

Figure S11: Comparison of the 633 °C - 700°C optimization with the 600 °C -700°C optimization. The 633 °C - 700 °C optimization is able to better reproduce all trends as well as the exact values. Therefore, the 633 °C – 700 °C optimization is used in the main manuscript.

Comparison of the 600°C optimization with the 600 °C - 700°C data sets

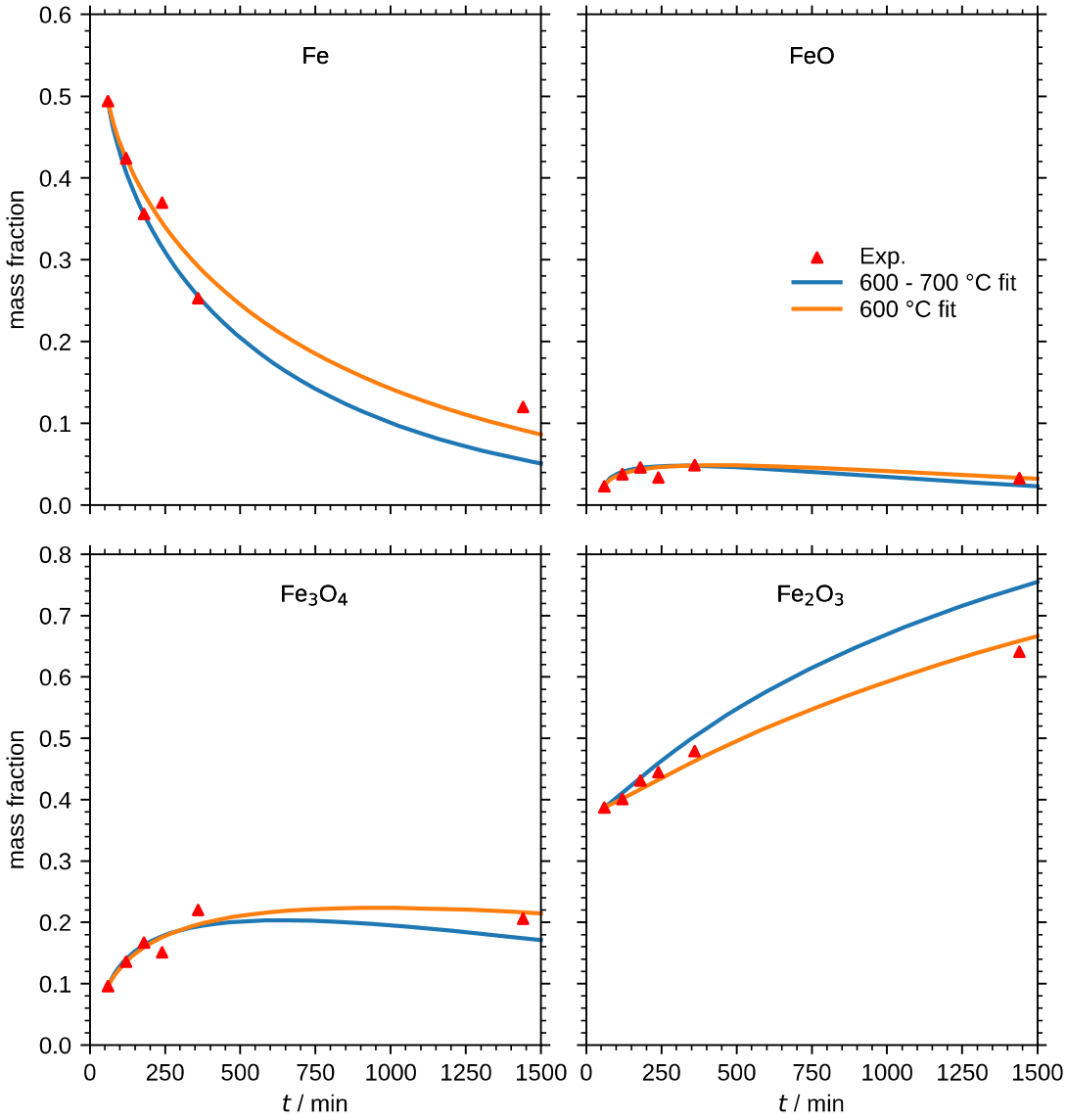

Figure S12: Comparison of the 600°C optimization with the 600 °C - 700°C optimization at 600 °C. The 600 °C optimization better represents the trends of all species. Since the optimization is only based on one temperature no activation temperature and pre-exponential factor can be extracted.

Comparison of the oxidation behavior of a mono dispersed particle distribution (Sauter mean diameter) with the one of the real particle size distributions.

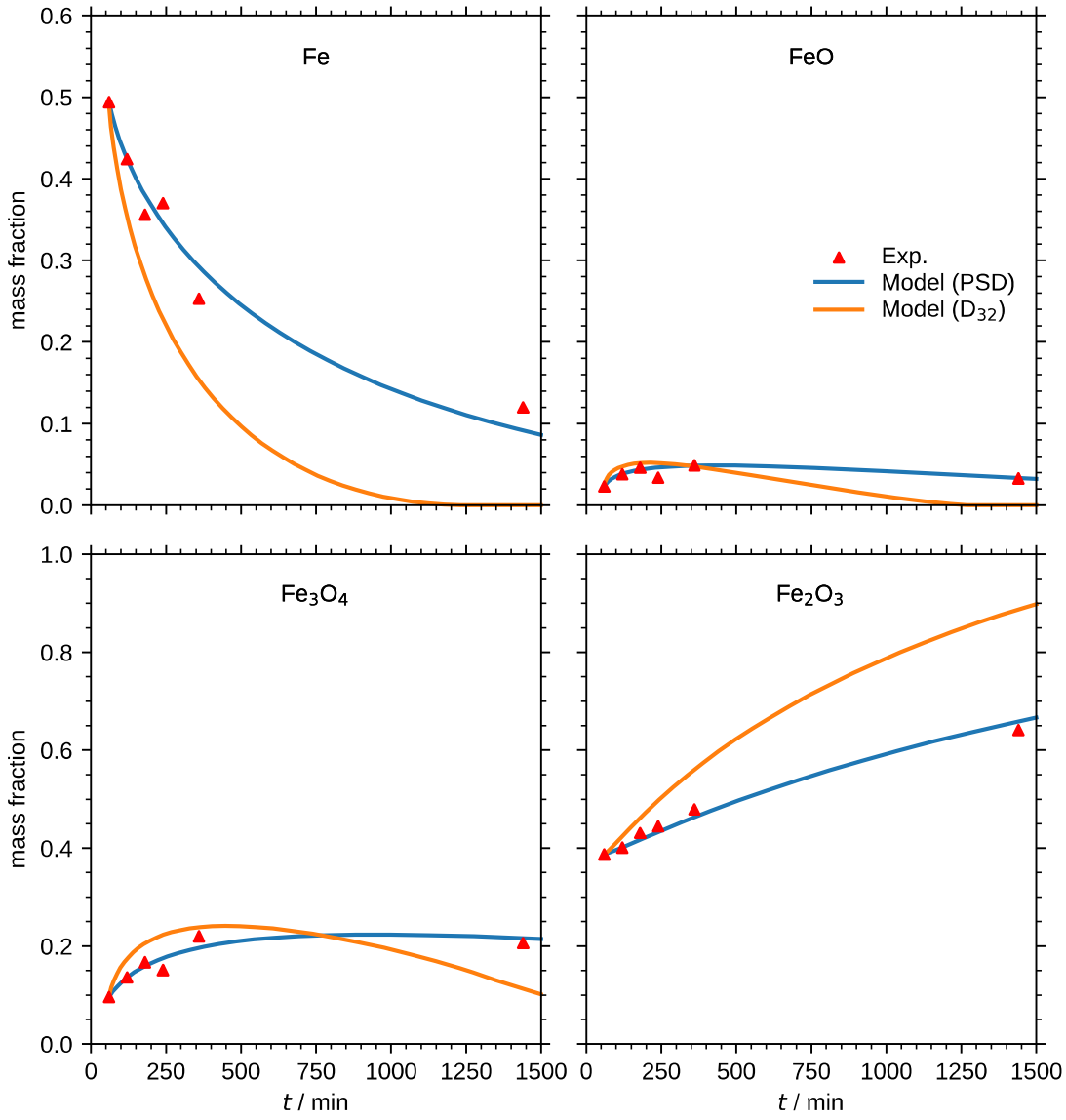

Figure S13: Comparison of the oxidation behavior of a mono dispersed particle distribution (Sauter mean diameter) with the one of the real particle size distributions. It becomes apparent that the oxidation behavior of a monodisperse distribution with the mean Sauter diameter behaves differently than a fully dissolved PSD. For this reason, the full PSD is taken into account for all further simulations.

Particle size over the volume-based probability colored by mass fraction and mass fraction for each particle size (600 °C optimization).

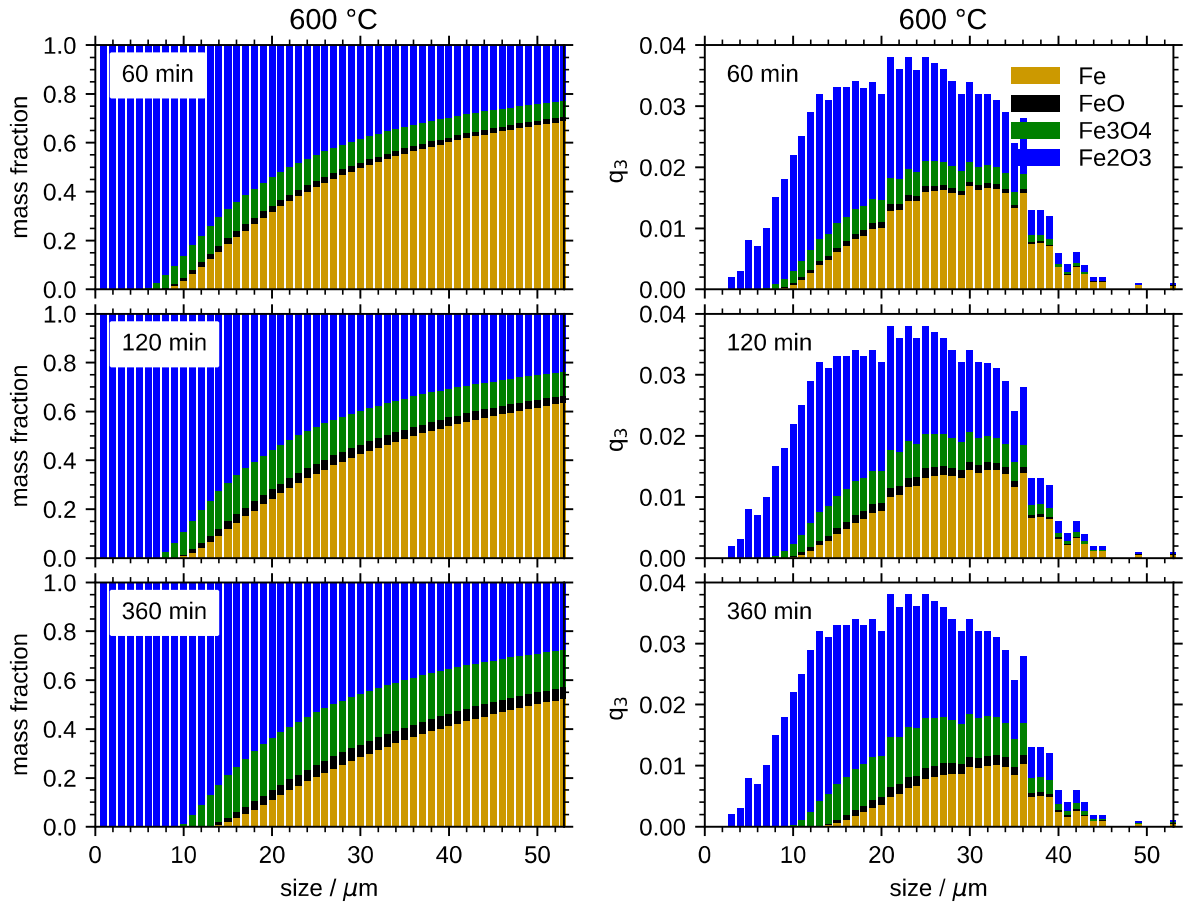

Figure S14: Particle size over the volume-based probability colored by mass fraction (right) and mass fraction for each particle size (left) (600 °C optimization).

Particle size over the volume-based probability colored by mass fraction (633 °C – 700 °C optimization).

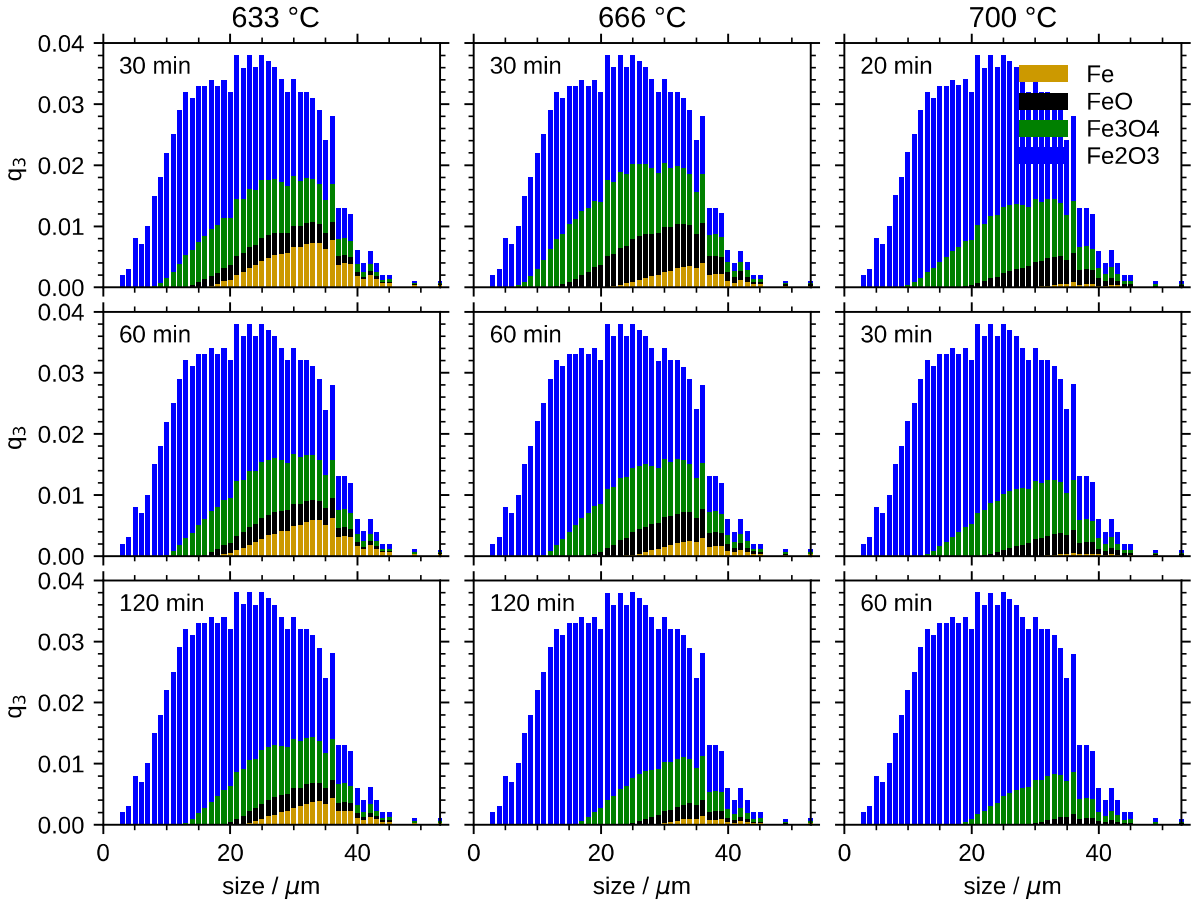

Figure S15: Particle size over the volume-based probability colored by mass fraction (633 °C – 700 °C optimization). The first row represents the initial state in the parabolic region. The second and third row are based on the simulations with the 633 °C -700 °C optimization. It is shown that with increasing oxidation state more of the smaller particles are fully converted and less particles are participating in the reaction.

Species mass fraction for each particle size (633°C-700 °C optimization).

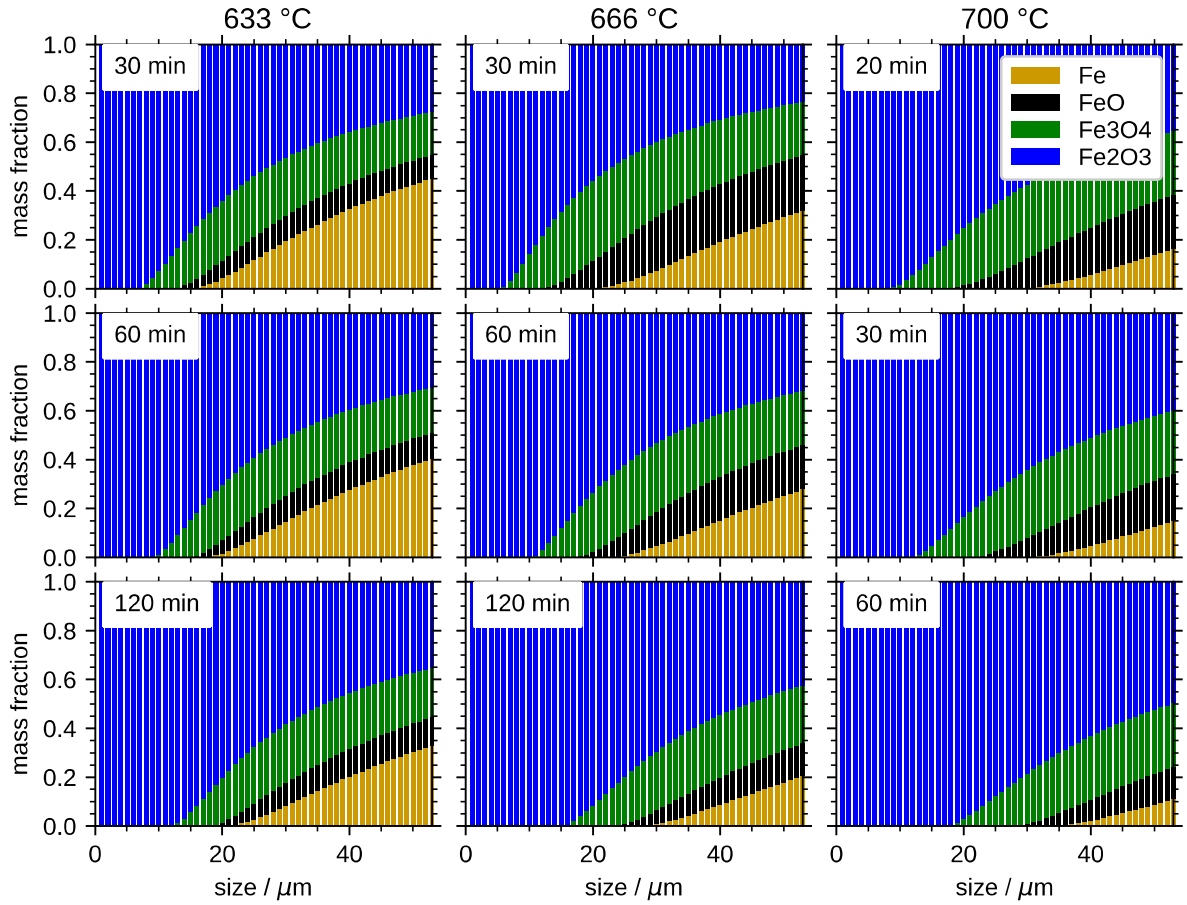

Figure S16: Species mass fraction for each particle size (633°C-700 °C optimization). Compared to the previous plot here the mass fraction of the different particles can be more easily be compared. Even though all particles are initialized with the same layer thickness the mass fractions vary strongly based on the particle size.